Low Infant Functional Connectome-based Identification Rates Across the First Year of Life

Alexander J. Dufford[a], Stephanie Noble[b], Siyuan Gao[e], and Dustin Scheinost[a,b,c,d]

[a]Child Study Center, Yale School of Medicine, New Haven, CT, USA

[b]Department of Radiology and Biomedical Imaging, Yale School of Medicine

[c]Department of Statistics and Data Science, Yale University, New Haven, CT, USA

[d]Interdepartmental Neuroscience Program, Yale University, New Haven, CT, USA

[e]Department of Biomedical Engineering, Yale University, New Haven, CT, USA

* Correspondence should be addressed to:

Alexander J. Dufford, Ph.D.

Yale Child Study Center

230 S Frontage Rd

New Haven, CT 06519, USA

Email: alexander.dufford@yale.edu

Abstract

The uniqueness and stability of the adolescent and adult functional connectome has been demonstrated to be high (80–95% identification) using connectome-based identification (ID) or "fingerprinting". However, it is unclear to what extent individuals exhibit similar distinctiveness and stability in infancy, a developmental period of rapid and unparalleled brain development. In this study, we examined connectome-based ID rates within and across the first year of life using a longitudinal infant dataset at 1 month and 9 months of age. We also calculated the test–retest reliability of individual connections across the first year of life using the intraclass correlation coefficient (ICC). Overall, we found substantially lower infant ID rates than have been reported in adult and adolescent populations. Within-session ID rates were moderate and significant (ID = 48.94–70.83%). Between-session ID rates were very low and not significant, with task-to-task connectomes resulting in the highest between-session ID rate (ID = 26.6%). Similarly, average edge-level test-retest reliability was higher within-session than between-session. These findings suggest a lack of uniqueness and stability in functional connectomes across the first year of life consistent with the unparalleled changes in brain functional organization during this critical period.

Key words: fingerprinting, brain development, resting-state, test–retest reliability, connectomics

Introduction

The first year of life is marked by rapid and unparalleled rates of brain development (Gao, Lin, Grewen, & Gilmore, 2017; Holland et al., 2014). Across the first year of life, functional networks mature towards 'adult-like' connectivity patterns from primary and secondary visual networks, to higher order networks such as the dorsal attention network and default mode network (Gao, Alcauter, Elton, et al., 2015; Gao, Alcauter, Smith, Gilmore, & Lin, 2015). While functional connectivity is rapidly developing in infancy, it has been found to be both unique and stable in adults (Finn et al., 2015; Horien et al., 2018) and adolescents (Horien, Shen, Scheinost, & Constable, 2019; Jalbrzikowski et al., 2019; Kaufmann et al., 2017). This uniqueness and stability in adulthood has been demonstrated using connectome-based identification or "fingerprinting", a procedure which uses functional connectomes to identify an individual from a pool of other individuals based upon the similarity of connectomes from separate sessions. Examining the uniqueness and stability of the infant functional connectome has the potential to provide insight into how the functional connectome develops its individual variability (Finn et al., 2015). Given the rapid and dynamic changes to the brain's functional architecture during this period (Gao, Alcauter, Smith, et al., 2015; Gao et al., 2017; Zhang, Shen, & Lin, 2019), understanding the development of its individual variability may be useful for understanding both typical and atypical neurodevelopment. Studies using this connectome-based identification procedure have found identification rates between 80–95% in adults and adolescents (Finn et al., 2015; Horien et al., 2018; Horien et al., 2019; Jalbrzikowski et al., 2019; Kaufmann et al., 2017). However, it is unclear if high identification rates are achievable in infancy when functional connectivity is undergoing extensive development.

A complementary approach is to examine the stability of individual connections, or edges. In adults, edge-level test-retest reliability via the intraclass correlation coefficient (ICC) is typically low despite high ID rates using the full connectome (Noble et al., 2017). A recent study of test–retest reliability in infants provides evidence that edge intraclass correlation for infants is low (Wang et al., 2020). However, this study only included resting-state data, tested within-session test–retest reliability and did not conduct connectome-based identification. In this study, we expand upon these findings and examine test–retest reliability for both resting-state and task-based data as well as between-session test–retest reliability.

We examined these questions using data from infants that have both resting-state and task data (native language task) at 1–2 months and at 9–10 months. We hypothesized between-session connectome-based identification with functional connectomes calculated from resting-state data would be poor ID rates below 50%; further, we hypothesized between-session identification based upon task data would be fair (60–80%) but not as high as adult studies (90%). We hypothesized that within-session ID would be higher than between session and overall higher in the task-based data. Regarding the test–retest reliability of the functional connectivity data, we hypothesized that edge intraclass correlation coefficients would be poor for both between-session resting-state and task-based data connectomes with task-based data being slightly higher. We predicted edge intraclass correlation coefficients would be higher for both within-session resting-state and task-based data, with task-based data being higher. Lastly, studies in adults and adolescence have found frontoparietal connections contribute most to successful identification. While these connections are immature in infancy, we hypothesize the immature connectivity of frontoparietal connectivity will still contribute most to successful identification with more mature patterns of connectivity being associated with higher success of identification.

1. Methods and Materials

1.1. Infant participants. Infant data for this study were acquired from the National Database for Autism Research (NDAR). The dataset identifier is NDARCOL0002026 (Susan Bookheimer). This study used longitudinal neuroimaging in infancy to examine early markers of Autism Spectrum Disorder (ASD). Infants were recruited in two categories: Low Risk (LR) and High Risk (HR). HR was defined as the infant having at least one older sibling with a confirmed diagnosis of ASD. Infants were categorized as HR if they had no family history of ASD defined as no first- or second-degree relatives with ASD or another neurodevelopmental disorder. Participant exclusionary criteria included: genetic or neurological condition, perinatal condition impacting development, visual, hearing, or motor impairment, and MRI contraindication. Infants were full-term and had births without complications and normal birth weight (>3000 g). At Session 1 (1.5 months), 74 infants were scanned (41 HR, 33 LR); however, 4 HR and 1 LR did not complete the scan. At Session 2 (9 months) 78 infants were scanned (48 HR, 30 LR); however, 7 HR and 5 LR infants did not complete the scan. Infants at Session 1 and 2 were scanned during rest (naturally sleep with no task) and task (native language task); however, the infants that completed these sessions successfully and had usable data varied between scan type (rest or task) and session. Two infants (HR) were removed from the analysis as testing with the ADOS indicated moderate to severe concern for ASD. For the between-session analyses (connectome-based identification and test–retest reliability) there were n = 27 for Rest1–Rest2 (had usable data at rest session 1 and rest session 2) and n = 15 for Task1–Task2. For Rest1–Task2 there were n = 24 with usable data, and n = 17 for Task1–Rest2. For the within-session analyses, there were n = 24 for Rest1–Task1 and n = 47 for Rest2-–Task2. See **Table 1** for more details about the sample. This study was approved by the Institutional Review Board of the Yale School of Medicine. The data used for the study is available at https://nda.nih.gov/. In post-

analysis, we examined if successful identification varied by ASD risk status (low risk versus high risk) or infant sex (male versus female) using two Pearson's chi-square test with Yate's correction for continuity. The Yate's correction is suggested when analyzing a 2x2 contingency table if one of cell frequencies is below 10.

Table 1. Demographic information for the sample.

Variable	Sample (n = 55)
Sex (1)	33 (60%)
Risk (1)	28 (50.91%)

Male = 1, High risk for autism spectrum disorder

1.2. Infant MRI acquisition. Infant MRI data were acquired using a 3T Siemens Tim Trio and 3T Siemens Prisma; data were acquired using a 12-channel head coil for the Tim Trio scanner, and a 32-channel head coil for the Prisma scanner. High resolution T2-weighted echo planar structural images were acquired (TR = 5000 ms, TE = 28 ms, FOV = 192, 34 slices, 128 x 128 matrix, 1.5 mm in-plane resolution, 4mm-thick axial slices for the Tim Trio, all identical parameters for the Prisma except for 33 slices were acquired and TE = 45 ms). Resting-state acquisitions were 8 minutes in duration using a T2*-weighted echo planar imaging sequence (TR = 2000 ms, TE = 28 ms, 64 x 64 matrix, FOV = 192 mm, 34 slices, 3 mm in-plane resolution, 4 mm-thick axial slices. Native language task data were acquired with a T2*-weighted echo planar imaging sequence (TR = 3000 ms, TE = 28 ms, 56 x 56 matrix, FOV = 192 mm, 34 slices, 4 mm thick for the Tim Trio, and all parameters were identical for the Prisma except for 33 slices were acquired) 7.2 minutes in duration (144 volumes).

Resting-state and native language task data were collected from infants during their natural sleep. Participants put their infant to sleep during their regular bedtime. Once asleep, the swaddled infants were transferred into the scanner. Infants were fit with earplugs and MiniMuffs (Natus Medical Inc., San Carlos, California) for hearing protect as well as headphones to convey the auditory stimuli during the native language task. Infants were laid in a custom-made bed which could fit inside the head coil and was secured to the scanner bed with Velcro. A weighted blanked and foam pads were used to minimize infant head motion. A staff member of the study remained inside the scanner room to monitor large infant motion, waking, or signal of distress i.e. crying. For the native language task, infants heard speech stimuli from different female native speakers of English and Japanese. Infants heard 7 segments in each language that were matched on duration, intensity, peak amplitude, pitch, and pitch range. The native language task used a traditional block design with alternating streams of English and Japanese speech (18 seconds in duration) interleaved with blocks of silence (12 seconds in duration). Infants heard the speech through the MRI-compatible headphones.

1.3. Infant functional connectivity processing. Resting-state and native language task data underwent motion correction using SPM8 (http://www.fil.ion.ucl.ac.uk/spm/). Images were iteratively smoothed using AFNI's (http://afni.nimh.nih.gov/afni/) 3dBlurToFWHM to reach a smoothness of approximately 8 mm full-width half maximum (FWHM). Linear and quadratic drifts, mean cerebrospinal fluid signal, mean white matter signal, and mean gray matter signal were regressed from the data. Additionally, a 24-parameter motion model was regressed from the data. The 24-parameter motion model includes six rigid-body motion parameters, six temporal derivatives, and these terms squared. The functional data was temporally smoothed with a Gaussian filter with an approximate cutoff frequency = 0.12 Hz. Gray matter, white matter, and

cerebrospinal fluid masks were defined on the reference brain and a dilate gray matter mask was applied to include on voxels within gray matter for further calculations. As motion has been shown to be an important confound in functional connectivity studies, the frame-to-frame displacement averaged across the functional volumes was calculated for each session of resting-state and the native language task. Infants were excluded from the analysis if their average frame-to-frame motion was greater than 0.15 mm for one of the scan types for that ID calculation. For Rest1–Task1, 15 infants were excluded due to motion, 4 for Rest2–Task2, 1 for Rest1–Rest2, 3 for Rest1–Task2, and 8 for Task1–Rest2.

1.4. Infant connectivity matrices. Connectivity matrices were calculated using an infant-specific parcellation which consisted of 95 nodes providing whole brain coverage (Scheinost et al., 2016). First, the parcellation was defined in the template space and then transformed back into each participant's individual space using a non-linear registration (Joshi et al., 2011). The mean time-course for each of the nodes was calculated and correlated with each other using a Pearson correlation. After excluding nodes that had missing data, each participant had an 83 by 83 connectivity matrix. Correlations were normalized to *Z* scores using a Fisher transformation.

1.5. Adult (HCP 900) dataset. To compare patterns of differential power (edges to contribute most to successful identification) and test–retest reliability, we utilized adult data from the Human Connectome Project, HCP 900 subjects release (Van Essen et al., 2013). Data were preprocessed and connectivity matrices were calculated using a previously described analysis pipeline (Finn et al., 2015, 2017; Shen et al., 2017). However, to match the infant connectivity matrices, connectivity matrices in the adult were calculated using the 95-node infant atlas registered into adult MNI space rather than the Shen-268 atlas. The adult MRI (HCP 900) data

acquisition details can be found in Ugurbil et al., (2013). For the adult resting-state data (HCP), the resting-state fMRI protocol has been previously described in detail (Glasser et al., 2013; Smith et al., 2013, Van Essen et al., 2013). Resting-state data was acquired on two days; for the current study Day 1 (left-to-right phase encoding) resting-state data was considered Session 1 and Day 2 resting-state data (left-to-right phase encoding) was considered Session 2 as described in Horien et al. (2018).

The adult resting-state data (HCP 900) were pre-processed and connectivity matrices were calculated as described elsewhere (Finn et al., 2015; Shen et al., 2017). Of the HCP 900, 835 resting-state scans had complete data for 'LR' phase encoding on both days (Session 1 and Session 2). To be able to directly compare the connectivity matrices between the infants and adults, the infant-specific parcellation (Scheinost-95) was registered into adult MNI space and connectivity matrices were calculated based upon this parcellation. This resulted in 83 by 83 connectivity matrices for the adult data. Participants were excluded from the analysis if their average frame-to-frame motion was greater than 0.15 mm. This resulted in 81 participants being excluded from the adult sample, resulting in 754 participants for the HCP 900 analyses.

1.6. Connectome-based identification procedure. The connectome-based identification procedure followed previous studies using this method (Finn et al., 2015; Horien et al., 2019) using scripts obtained from NITRC (https://www.nitrc.org/projects/bioimagesuite). This procedure consists of creating a database of all connectivity matrices for the dataset. Through an iterative process, each participant from a different session (Session 1 or Session 2) is denoted as the 'target'. The Pearson correlation between the target and all other matrices in the database is computed. A correct identification occurs when the highest Pearson correlation coefficient is between the target in one session and the same in the second session. This process is repeated

until each participant serves as the target once and is repeated for all participants, sessions, and database-target combinations. The connectome-based identification procedure results in two identification rates (ID rates). ID rate is tested across two possible configurations by exchanging the roles of target and database session. Identification rate (ID rate) is computed as the percentage of participants whose identity was correctly predicted out of the total number of participants. To examine if ID rates were above chance-level, permutation testing was used to generate a null distribution such that participant identities were shuffled at random and the ID rate was calculated with the random labels. The ID rates from using the correct labels were compared to the null distribution to test for significance. For between-session ID rates, Session 1 was data collected at the first time point (1–2 months old, resting-state or native language task) and Session 2 was data collected from the second time point (9–10 months old, resting-state or native language task). For within-session ID rates, either resting state data was selected as Session 1, the native language task was selected as Session 2 and vice versa. The Pearson correlation-based ID procedure was conducted using the raw connectivity matrices as well as connectivity matrices projected into tangent space. The ID procedure was conducted between all sessions and all scan types (resting-state and native language task).

1.7. Geodesic distance identification procedure. Using geodesic distance, rather than Pearson correlation, as the distance metric in the identification procedure in adults has been shown to achieve over 95% accuracy with resting-state data (Venkatesh et al., 2020). Geodesic distance is a distance metric that is non-Euclidean and considers the manifold on which the data lies. The Geodesic Distance ID procedure follows the same basic structure as the Pearson correlation-based ID procedure using the 1-Nearest Neighbor except that geodesic distance is computed as the distance measure rather than Pearson correlation. The geodesic distance

identification procedure was conducted for both raw connectivity matrices and for the tangent space connectivity matrices. As with the Pearson-based ID procedure, the geodesic distance ID procedure was conducted between all Sessions and all scan types (resting-state versus native language task). The geodesic distance ID procedure was implemented using code (https://github.com/makto-toruk/FC_geodesic) from the original geodesic distance ID study (Venkatesh et al., 2020).

1.8. Differential power analysis. For each of the ID rates that reached statistical significance via permutation testing we computed the differential power (DP) as described elsewhere (Finn et al., 2015). DP is an estimate for each edge of the likelihood that within-participant similarity is higher than between-subject similarity. DP is calculated as the product of the edge value from Session 1 and Session 2 from the same participant is compared to the project of the same edge value from Session and Session 2 from unmatched participants. If the within-participant product is higher than between-participant product across all the participants in the sample, this edge contributes highly to identification (indicated by a high DP value). DP was calculated for the infant data in which ID rates were significant and calculated for the adult (HCP 900) data.

1.9. Test–retest reliability analysis. To examine the role of test–retest reliability in connectome-based identification in the first year of life, we used the Generalizability Theory ICC toolbox (https://github.com/SNeuroble/Multifactor_ICC). Our analysis of test–retest reliability followed the generalizability theory (G theory) framework which has been used for test–retest reliability of functional connectivity in previous studies (Forsyth et al., 2014; Gee et al., 2015; Noble et al., 2017). First, the variance components for all factors are measured which include participants (the "object" of measurement and sessions/scan type ("facets") and their

interactions. The Generalizability Theory ICC toolbox uses an ANOVA model (3-way in this case) to estimate variance due to all factors using the MATLAB OLS-based function 'anovan'. For the model, negative variance components were small in their magnitude and set to 0 (Shavelson, Baxter, & Gao, 1993). Once variance components are estimated, test–retest reliability can be calculated. We calculated the "absolute reliability" that is measured by the dependability coefficient (D-coefficient). The D-coefficient is a form of intraclass correlation coefficient or ICC (Shrout & Fleiss, 1979) which is defined as the ratio of variance due to the object of measurement versus source of error. D-coefficients were calculated for each edge which was summarized by its mean and standard deviation across all edges of the brain. D-coefficients can be interpreted as <0.4 = poor; 0.4–0.59 = fair; 0.60–0.74 = good; and >0.74 = excellent (Cicchetti & Sparrow, 1981). Mean, standard deviations, and ranges for D-coefficients were calculated for all between all scan types (resting-state and native language task) and sessions (Session 1 and Session 2). To compare infant test–retest reliability to adult test-test reliability, we calculated the edge-level ICCs for the HCP data. We also examined the correlation between ICC and DP using a one-tailed Mantel test with 1000 iterations. The test was one-tailed as we hypothesized a positive correlation between ICC and DP.

2. Results

2.1. Connectome-based identification. Using the Pearson-based connectome ID procedure, we found support for our hypothesis that within-session ID rates would be highest (between 48.94% and 70.83%). However, ID rates for Session 2 were not substantially higher than Session 1 as hypothesized. Between-session ID rates were very low and mostly nonsignificant with the highest rate being for Task1–Task2 (26.67%). **Table 2** shows each ID rate for each task–rest pair for the Pearson-based ID procedure with the raw connectivity

matrices. Using the geodesic distance-based connectome ID procedure, ID rates were not substantially higher than the ID rates from the Pearson-based ID procedure (when the Pearson correlation coefficient is the distance measure rather than the geodesic distance, see **Table 3**). However, the geodesic distance-based ID rates follow a consistent pattern as the Pearson-based ID rates in that the highest ID rates are for the within-session identifications. Between-session ID rates remained very low and mostly nonsignificant. ID rates for the adult data was 71.6% and 71.4% consistent with previous studies examining ID rate in the HCP sample using the resting-state data (Horien et al., 2018). In adult connectome-based ID studies, ID rate improvements have been shown using geodesic distance as the distance measure rather than Pearson correlation (Abbas et al., 2021). We observed some improvements of the similar magnitude for the within-session ID rates, overall geodesic distance did not improve between-session ID rates.

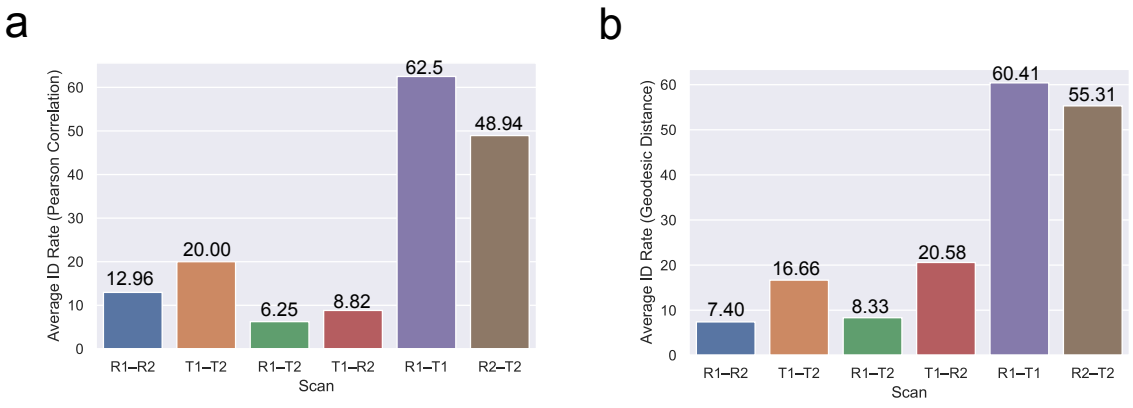

Figure 1. (a) Results of the Pearson connectome-based identification procedure. Bar plots show the average ID rates for each scan pair (R1–R2: Rest1–Rest2, T1–T2: Task1–Task2, R1–T2:

(Rest1–Task2), T1–R2: Task1–Rest2, R1–T1: Rest1–Task1, and R2–T2: Rest2–Task2. (b) Results of the geodesic distance connectome-based identification procedure.

Table 2. Results of the Pearson connectome-based identification procedure. ID Rate 1 and ID Rate 2 refer to the percentage of correct identifications (a participant Session 1 data was most highly correlated with themselves at Session 2) with Session 1 and Session 2 as target and database (respectively) for Rate 1 and reversed for Rate 2.

Scan Type (Pearson)	N	Average ID Rate	ID Rate 1	ID Rate 2	P-value (Rate 1)	P-value (Rate 2)
Rest1–Rest2	27	12.96	11.11	14.81	0.075	0.005*
Task1–Task2	15	20	26.67	13.33	0.004*	0.25
Rest1–Task2	24	6.25	8.33	4.17	0.27	0.65
Taskl–Rest2	17	8.82	5.88	11.76	0.67	0.27
Rest1–Task1	24	62.5	70.83	54.17	0.001**	0.001**
Rest2–Task2	47	48.94	48.94	48.94	0.001**	0.001**

Table 3. Results of the geodesic distance connectome-based identification procedure. ID Rate 1 and ID Rate 2 refer to the percentage of correct identifications (a participant Session 1 data was most highly correlated with themselves at Session 2) with Session 1 and Session 2 as target and database (respectively) for Rate 1 and reversed for Rate 2.

Scan Type (Geodesic Distance)	N	Average ID Rate	ID Rate 1	ID Rate 2	P-value (Rate 1)	P-value (Rate 2)
Rest1–Rest2	27	7.40	3.70	11.11	0.67	0.08
Task1–Task2	15	16.66	20.0	13.33	0.001**	0.001**
Rest1–Task2	24	8.33	8.33	8.33	0.27	0.25
Taskl–Rest2	17	20.58	23.52	17.64	0.001**	0.001**
Rest1–Task1	24	60.41	66.66	54.16	0.001**	0.005*
Rest2–Task2	47	55.31	55.31	55.31	0.001**	0.08

2.2. Differential power analysis. DP was calculated for each of the connectome-based ID rates ($p < 0.05$) (see **Figure 1**). The DP analysis focused on the DP for the two within-session ID rates (Rest1–Task1 and Rest2–Task2) for their relatively high ID accuracy. We included a DP analysis of Rest1–Rest2 to examine DP 'developmentally' as there was approximately 8 months between the two scans. As a comparison group, we also calculated DP for the adult data. Similar to previous studies (Finn et al., 2015; Horien et al., 2018; Horien et al., 2019), DP across infant and adult scans all included a widely distributed network of edges including the prefrontal, temporal, and parietal cortices. First, we examined if the DP edges were significantly different between adults and infants in terms of the number of significant prefrontal-to-prefrontal connections (PFC–PFC), prefrontal-to-non-prefrontal (PFC–nonPFC), and non-prefrontal-to-non-prefrontal connections (nonPFC–nonPFC) (see **Table 4** for count totals). Kolmogorov-Smirnov (K-S) tests indicated that the DP edge distributions for the PFC–PFC connections for Rest1–Task1, Rest1–Rest2, Rest2–Task2 and adult data did not follow a normal distribution (*ps*

< 0.001). A two sample K-S test indicated that there was no significant difference between the distributions for the adult data and Rest1–Task1 data for PFC–PFC DP edges ($D = 0.01$, $p < 0.99$), PFC–nonPFC DP edges ($D = 0.02$, $p < 0.99$) and nonPFC–nonPFC DP edges ($D = 0.05$, $p < 0.99$). The same patterns were observed using two sample K-S test for the Rest1–Rest2 data (all ps > 0.05), and the Rest2–Task2 data (all ps > 0.05). These findings suggest that the distributions of DP edges were not differing between adults and infants.

Table 4. Number of differential power (DP) edges ($p < 0.05$) for each connectome-based ID rate.

Scan	PFC– PFC	PFC–nonPFC	nonPFC–nonPFC
Infant Rest1–Task1	8	56	81
Infant Rest1–Rest2	6	52	91
Infant Rest2–Task2	12	65	84
Adult Rest1–Rest2	9	62	80

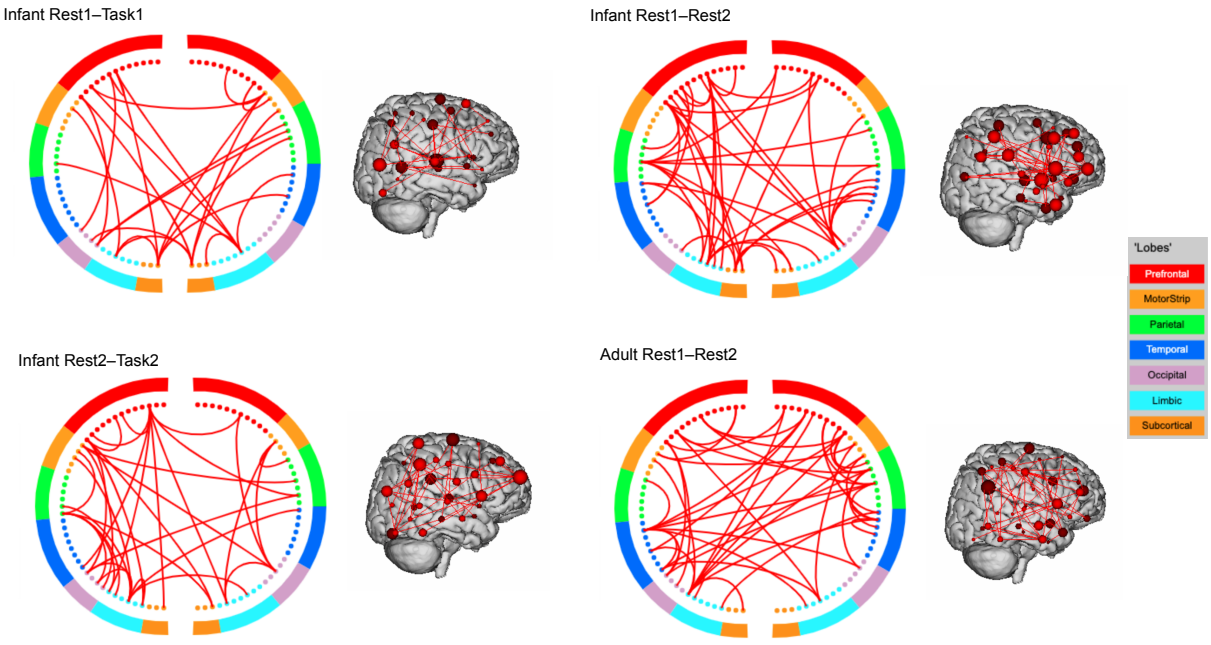

Figure 2. Circle plots showing the significant differential power (DP) edges for each connectome-based identification at $p < 0.05$. For visualization purposes, a degree threshold of 7 was applied.

Second, we examined if there was a developmental shift of the degree distribution towards higher degree nodes in the prefrontal cortex with the highest being the adult DP data. We calculated the degree for each of the DP matrices and examined if degree distributions were significantly different between adults and infants. A two sample K-S test indicated that there was no significant difference between the degree distributions, across the brain, for the adult data and Rest1–Task1 ($D = 0.03$, $p < 0.99$), adult data and Rest1–Rest2 ($D = 0.04$, $p < 0.99$), and adult data and Rest2–Task2 ($D = 0.02$, $p < 0.99$). These findings suggest that the degree distributions of DP edges were not differing between adults and infants.

Lastly, we examined if the low ID rates in infants may be due to differences in the underlying functional connectivity across the frontoparietal network (as this network has a protracted developmental trajectory (Fair et al., 2007; Gao, Alcauter, Smith, et al., 2015; Peters, Van Duijvenvoorde, Koolschijn, & Crone, 2016) and contributes highly to adult ID rates (Finn et al., 2015; Jalbrzikowski et al., 2019)). For the infant (Rest1–Task1, Rest1–Rest2, and Rest2–Task2) and adult data, we calculated the average functional connectivity across the frontoparietal network (8 nodes) and examined differences between adults' and infants' functional connectivity. Using a permutation with 1000 iterations, adult frontoparietal functional connectivity (averaged across Rest1 and Rest) was significantly different than infant frontoparietal functional connectivity (averaged across sessions) for Rest1–Task1 ($t = -0.028$, $p < 0.001$), Rest1–Rest2 ($t = -0.022$, $p < 0.001$), and Rest2–Task2 ($t = -0.017$, $p < 0.001$). There were

no significant differences in frontoparietal functional connectivity among the infant data (*p*s > 0.05). The mean frontoparietal functional connectivity for the adults was -0.03 therefore the negative observed differences between the adults and infants (mean for Rest1–Task1 = -0.0013, mean for Rest1–Rest2 = -0.0080, mean for Rest2Task2 = -0.0128) suggest a developmental shift towards more 'negative' functional connectivity across the frontoparietal network (with Rest2–Task2, when infants are oldest, showing the least difference from the adult data). Overall, these findings suggest that differences in the underlying functional connectivity may be driving successful identification.

2.3. Analysis of successful identifications. For the connectome-based ID rates that were significant (Rest1–Task1, Rest2–Task2, Rest1–Rest2 (Rate 2), Task1–Task2 (Rate 1), we conducted a follow-up analysis of successful IDs. For Rest1–Task1, the chi square test indicated that successful ID was not found to vary according to infant risk status for ASD ($p < 0.10$) or infant sex ($p < 0.20$) for Rate 1. For Rest1–Task1 Rate 2, Rest2–Task2 (both rates), Rest1–Rest2 (Rate 2), Task1–Task2 (Rate 1), successful ID did not vary according to infant risk status for ASD or infant sex (all *p*s > 0.05).

2.4. Test–retest reliability. The means, standard deviations, and ranges for the D-coefficients for each rest-task combination (both sessions) based upon Pearson correlation are presented in (see **Table 5**, plotted on the brain in **Figure 2**, and as matrices sorted by lobe in **Figure 3**). For the Pearson-based correlation matrices, within-session mean edge-level D-coefficients (ICC) are consistently higher than between-session mean edge-level D-coefficients. For both types of connectivity matrices, between-session mean edge-level D-coefficients consistently low (mean ~0.08). Within-session mean edge-level D-coefficients were consistently higher for Session 2 when the infants are 9–10 months old versus Session 1 when the infants are

1–2 months old. For both types of connectivity matrices, between-session mean edge-level D-coefficients were not higher for task-based versus resting-state matrices, which was not expected. Overall, across all of the rest-task and session comparisons, the mean edge-level D-coefficients were in the poor range. However, for both types of connectivity matrices, maximum values reached to 'good' or 'excellent' range for ICC. For the adult data, the ICC had a mean of 38 ± 0.12 and a range of 0.04–0.81.

Table 5. Means, standard deviations, and ranges of the D-coefficient (edge-level intraclass correlation coefficient) for each rest-task and Session combination (Rest1 = resting-state Session 1, Task1 = task Session 1, Rest2 = resting-state Session 2, Task2 = task Session 2) for Pearson correlation connectivity matrices.

Scan Type	N	ICC (Mean ± SD)	Range
Rest1–Rest2	27	0.09 ± 0.11	0 – 0.64
Task1–Task2	15	0.14 ± 0.15	0 – 0.77
Rest1–Task2	24	0.08 ± 0.11	0 – 0.55
Taskl–Rest2	17	0.09 ± 0.13	0 – 0.68
Rest1–Task1	24	0.19 ± 0.16	0 – 0.80
Rest2–Task2	47	0.16 ± 0.13	0 – 0.65

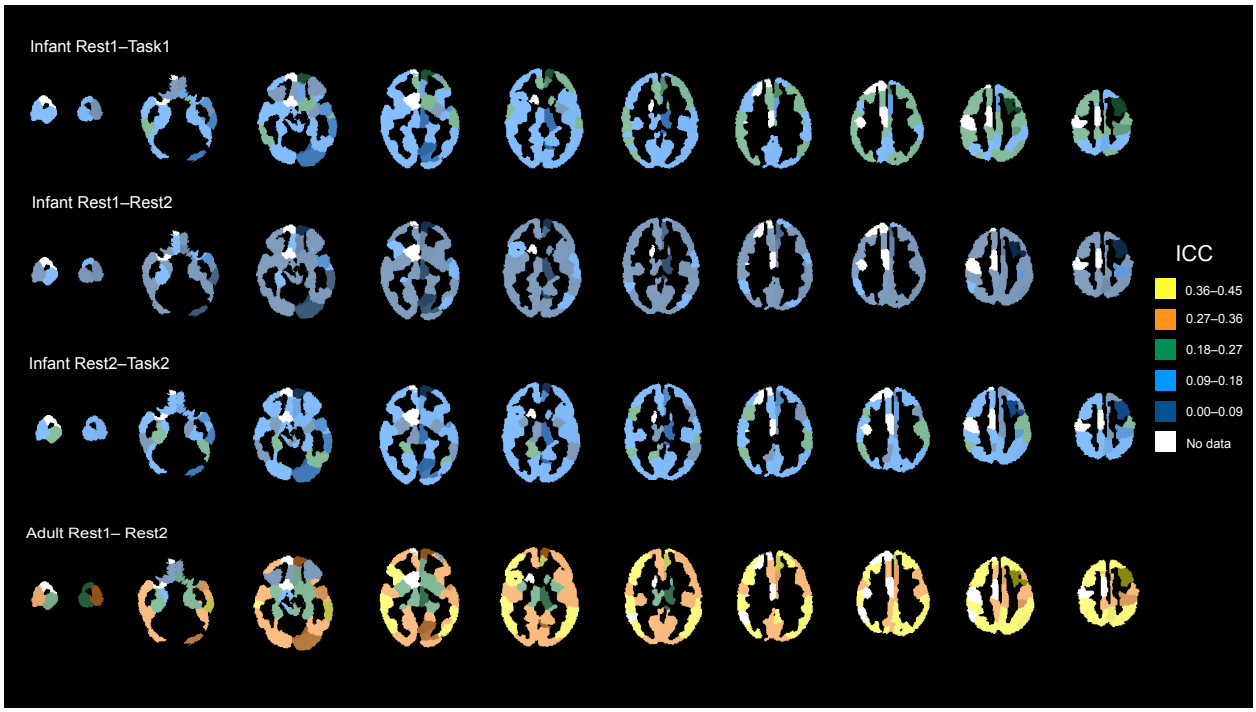

Figure 3. Mean intraclass correlation coefficient (ICC) for each region of the Scheinost-95 parcellation for infants and adults.

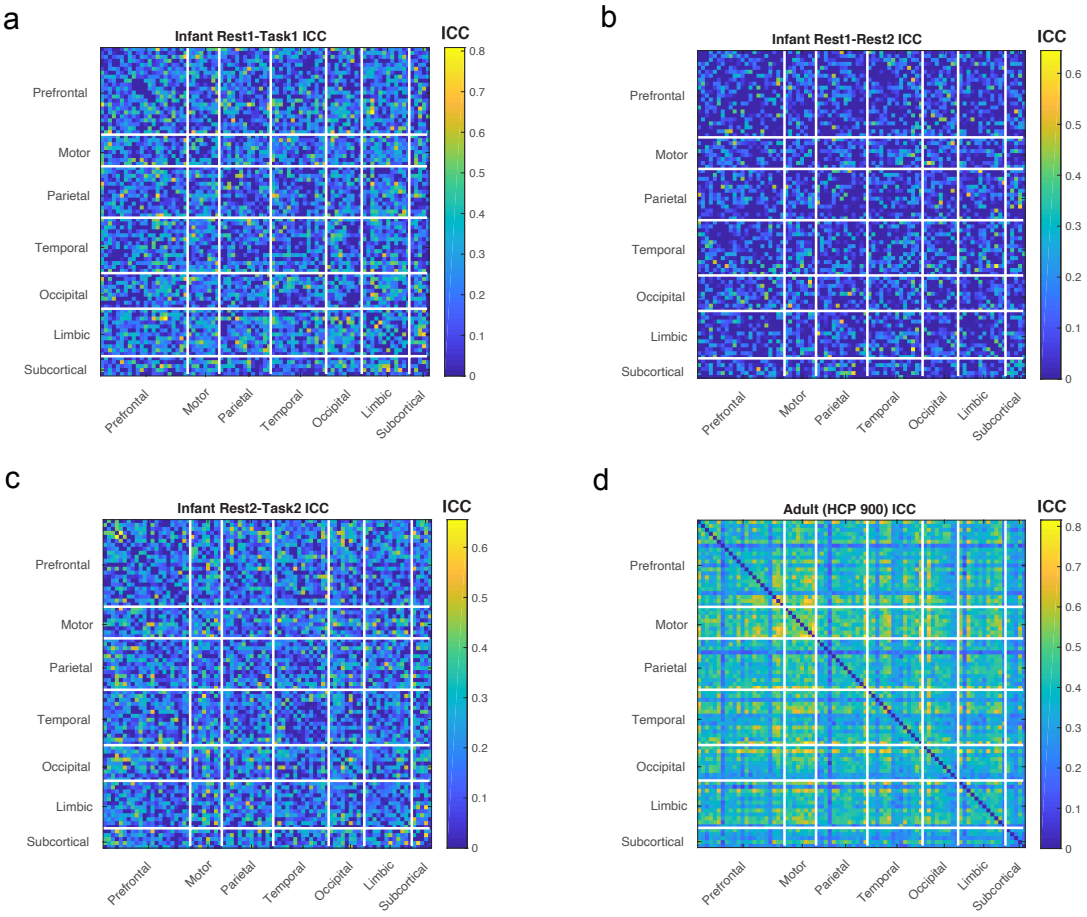

Figure 4. (a) Intraclass correlation coefficients (ICCs) organized by lobe for the infant Rest1–Task1 (b) ICCs organized by lobe for the infant Rest1–Rest2 (c) ICCs organized by lobe for the infant Rest2–Task2 (d) ICCs organized by lobe for the adult data (Rest1–Rest2 for the HCP 900 data).

We examined the correlation between ICC matrices for the infants and adults focusing on the two within session ID rates (Rest1–Task1 and Rest2–Task2) and the resting-state between-session ID rate (Rest1–Rest2). To examine the correlations between the matrices, we used a Mantel test (Mantel, 1967) with 1000 iterations. The Mantel test indicated Rest1–Task1 ICC

values for the infants were positively correlated with the adult ICC values ($r = 0.19$, $p < 0.001$). A positive correlation was also found between the adult ICC values and infant Rest2–Task2 ICC values ($r = 0.18$, $p < 0.001$). However, there was not a significant association between the adult ICC values and the infant Rest1–Rest2 ICC values ($p < 0.21$).

We examined if there was a significant difference between the ICC values for the adults and infants. Using a permutation test with 1000 iterations, we found that the ICCs for the adult data were significantly greater than the infant Rest1–Task1 data ($t = 0.17$, $p < 0.001$), infant Rest1–Rest2 ($t = 0.28$, $p < 0.001$), infant Rest2–Task2 ($t = 0.20$, $p < 0.001$). The ICCs for the infant Rest1–Rest2 data were lower than the infant Rest2–Task2 ($t = 0.07$, $p < 0.001$) and infant Rest1–Task1 data ($t = -0.10$, $p < 0.001$). However, there were no significant differences between the Rest1–Task1 and Rest2–Task2 data ($p < 0.99$). Together, these results suggest that, while the infant connectome exhibits lower ICC than the adult connectome, similar edges have higher ICC values in infants and adults.

2.5. Associations between test–retest reliability and differential power. We conducted a correlation analysis to examine if there was a correlation between edge-level test–retest reliability (ICC) and DP using a Mantel test with 1000 iterations (one-tailed). This was conducted to determine if edges that were the most reliable were the same edges that contributed highly to a successful identification. In all cases, the correlations between the DP and ICC were small ($r < 0.04$).

3. Discussion

In this study, we show that unlike in adulthood and adolescence, the infant functional connectome has low connectome-based identification rates across the first year of life. As

connectome-based identification rate has been used to quantify the uniqueness and stability of the functional connectome, the results suggest that infants do not yet possess the uniqueness and stability they will have later in development. Results showed that within-session ID rates were consistently the highest (48.94–70.83%) with lower ID rates for the between-session analyses (between 14.81–26.67%). As it may be related to ID rate, we also conducted a test–retest reliability analysis and found consistent results in which mean ICC's for within-session functional connectome edges were higher (0.16–0.19) while between-session functional connectome edges were consistently lower (0.09–0.14). Further, we found that functional connectome edges in infancy have lower ICC's than adults, however; similar edges have high ICC for infants and adults. These findings have implications for longitudinal studies using fMRI in the first year of life and suggest poor test–retest reliability. The findings show low stability and uniqueness of the functional connectome in infancy and suggest this may be due to the rapid and unparalleled brain development occurring this developmental period.

It could be hypothesized that the low connectome-based identification rates across infancy were due to poorer test–retest reliability (less reliable data in infants). However, we did not find support for a correlation between edge-level ICC and DP for the infants. This finding suggests that high DP edges for the infants are not simply edges that have greater test–retest reliability. This finding, along with the lack of findings for differences in DP, indicate across development similar edges are involved in successful identification, but these are not necessarily the edges with the highest test–retest reliability. This also suggests that the differences observed in infant versus adult ID rates are likely to be developmental changes and not simply due to increases in data quality.

Since the publishing of the first connectome-based identification study (Finn et al., 2015), there has been an interest in quantifying the uniqueness and stability of individual variability in the functional connectome developmentally. Two studies have shown high ID rates in adolescence (Horien et al., 2019; Jalbrzikowski et al., 2019) and one study found connectome-based ID rates increased between ages 8 to 22 with large increase during puberty (14.5 years old) (Kaufmann et al., 2017). Of particular relevance, both studies in adolescence, found that for adolescence, the functional connectome had high ID rates across periods of approximately a year (Horien et al., 2019; Jalbrzikowski et al., 2019). This finding demonstrates high ID rates across a similar range of time as the current study; suggesting that the higher ID rates observed were due to functional connectomes being more developmentally mature in adolescence. The findings from Kaufmann et al., show that 'connectome distinctiveness' continues to develop across adolescence. However, it was unclear if high ID rates were achievable from a large age range of 0–8 years old. Studies have quantified rates and development of both the structural and functional development of the brain and highlighted the first year of life as both rapid and unparalleled (Gao et al., 2017; Holland et al., 2014). The results of the current study suggest that for both resting-state and task-based data, average within-session connectome-based ID rates are low (below 65%). This pattern suggests that within a session, an infant's resting-state functional connectome is more highly correlated with its task functional connectome (and vice versa) for about half of the sample. This suggests that even within a session, an infant's resting-state (or task) connectome is being misidentified and has a higher correlation with another infant's connectome. For between-session ID rates, greater than 70% of the sample was being misidentified (higher correlation with another individual) for both resting-state and task data.

These findings that for the majority of infants in the study, the uniqueness and stability of the functional connectome has not been fully established.

We did not observe improvements in within-session ID rates (actually lower ID rates) when geodesic distance was used as the distance measure of functional connectivity instead of Pearson correlation (Abbas et al., 2021). The geodesic distance method captures the underlying non-Euclidean geometry of connectivity matrices (Abbas et al., 2021), this structure in the connectivity matrix may not be developed enough in infancy (or too noisy) to benefit ID rates. Across the Pearson and geodesic distance ID rates, between-session ID rates were consistently low (below 30%) with within-session ID rates between 40–60%. Future studies will be needed to examine if methods beyond the Pearson and geodesic distance-based ID procedures can achieve high ID rates across the first year of life. We also examined if ID rate varied due to infant sex or ASD risk status. We did not have find evidence for sex-specific effects for ID or that ID rate differed between high risk and low risk infants.

As connectome-based identification is a measure of multivariate test–retest reliability, we calculated the ICC of the edges of functional connectomes across scan (resting-state versus task) and age (1 month and 9 months). Whether between-session or within-session, mean edge ICC values were in the poor range for the infant data. As a comparison, mean edge ICC values were still in the poor range (0.37) but close the threshold of being considered fair (0.40)(Cicchetti & Sparrow, 1981) and similar to a meta-analysis of 25 resting-state studies that found an average edge-level ICC of 0.29 (Noble, Scheinost, & Constable, 2019). A recent study found similar results in infants (mean postmenstrual age of 45.14) (Wang et al., 2020), with within-session edge-level ICCs between 0.14–0.18. However, this study did not calculate between-session

ICCs. These findings suggest that even within-session, infant edge-level ICCs are extremely low and even lower across the first year of life. These findings have implications for future studies examining the infant functional connectome (especially longitudinally) and should be considered when design infant fMRI studies and interpreting results of studies.

We did not find support of our hypothesis that task-based data would have higher edge ICC's than resting-state data. This may be due to infants being asleep during both rest and the task. Further analysis of the edge-level ICCs showed a pattern of adult ICCs being higher than all of the infant ICCs, infant Rest1–Rest2 ICCs being lower than all of the other ICCs (infant and adult), and no significant difference between the infant Rest1–Task1 and Rest2–Task2. The Rest1–Rest2 ICCs are consistent with the pattern that between-session ICCs have lower test–retest reliability, these data show it drop substantially across the first year of life and highlight the extensive development occurring during this period.

Connectome-based identification studies in adolescence and adulthood have consistently found the highest contributing edges (high DP) to successful identification were frontoparietal and medial frontal connections (Finn et al., 2015; Horien et al., 2019; Jalbrzikowski et al., 2019). As these connections are present but immature in infancy, it is unclear if high DP edges in infants would differ from adults. DP connectomes were remarkably similar in terms of connections with edges spanning the brain among infants and between adults and infants. We did not find significant differences in the distribution of edges or the degree distribution of edges between adults and infants. These findings suggest that the difference observed between adult ID and infant ID rate is not due to connections that are typically high DP (frontoparietal and medial frontal) being 'absent' in regard to not being developed enough in infancy to contribute to

fingerprinting. As these primarily prefrontal connections were not absent, we also tested if the count of DP edges between PFC–PFC, PFC–nonPFC, nonPFC–nonPFC were significantly different between infants and adults. The lack of significant difference confirms that the distribution of edges was not different between infants and adults., We examined if the difference in ID rate between infants and adults may be attributable to higher degree distribution in prefrontal nodes such that adults had more developed 'hubs' in prefrontal regions and this helped to achieve higher ID rates.

While the results suggest there was not a significant difference DP distribution or degree distribution of DP, we found that the underlying frontoparietal functional connectivity was significantly different in infants compared to adults. The pattern of results comparing adult to infant frontoparietal network connectivity showed a developmental shift towards more negative functional connectivity. Older infants (Rest2–Task2) had the lowest difference between infants and adults while the youngest infant (Rest1–Task1) had the greatest difference between infants and adults. This pattern towards greater negative frontoparietal functional connectivity has been shown in previous developmental studies; however these typically focus on cortical–subcortical connectivity changes developmentally and less is known about the development of functional connectivity within the frontoparietal network (Lee & Telzer, 2016; Vendetti & Bunge, 2014). In addition to having consistently high contributions to successful ID rates (Finn et al., 2015; Horien et al., 2019; Jalbrzikowski et al., 2019), the frontoparietal network has been shown to develop rapidly across the first year of life (Gao, Alcauter, Elton, et al., 2015; Gao, Alcauter, Smith, et al., 2015) and continue to development into childhood and adolescence (Barber, Caffo, Pekar, & Mostofsky, 2013; Kipping, Tuan, Fortier, & Qiu, 2017; Kolskår et al., 2018).

Therefore, the low ID rates in infants compared to adults may be attributable to the differences in overall functional connectivity across the frontoparietal network.

The current study is not without its limitations. First, all of the scans were conducted during the infant's natural sleep. It is not currently clear how sleep impacts connectome-based ID rate as all studies to data have been conducted in awake participants. Infant functional connectivity during sleep has been shown to most closely resemble adult functional connectivity during sleep (Mitra et al., 2017). Examining ID rates in sleeping adults may be a way to address this limitation as measuring sleep state for infants during scanning would be a large methodological challenged. Second, it will be critical to examine ID rates across infancy in further samples to ensure these findings are not sample specific. The sample was collected to be comprised of ~50% infants with high genetic risk for ASD. We attempted to mitigate this limitation by demonstrating that there was no significant difference in ID rates between low-risk and high-risk infants. Third, the amount of data per acquired for each infant relatively short (7–8 minutes) compared to 12 minutes of data per run collected for the HCP. As total scan length is important for ID rates (Horien et al., 2018), future studies will be needed to examine the impact of run length on ID rates in infancy. Fourth, the imaging sequences used for the data collection have been improved since the data collection (non-multiband sequences). Further, differences in the conditions between task and rest as well as the imaging parameters being difference may have impacted the results. However, a study has shown that the spatiotemporal resolution of the scan do not impact ID rates (Horien et al., 2018). However, it is unclear how these factors may have impacted test–retest reliability for infants.

4. Conclusions

The current study found low uniqueness and stability of the individual functional connectome across infancy. This suggests that individual variability of the functional connectome is high across infancy with even substantial variability within-session. We found that test–retest reliability (for both within- and between- sessions) is poor for infants with the poorest ICCs found for within-session infant scans. Overall, these findings suggest that individual variability in the functional connectome is high early in development and that low identification rates across this period likely reflect the rapid and expansive brain development occurring during this time.

Acknowledgements

The current study was supported by National Institutes of Health Grant: T32MH18268 (AJD).

Disclosures

The authors report no biomedical financial interests or potential conflicts of interest.

Declaration of Competing Interest

The authors declare that they have no known competing financial interests or personal relationships that could have appeared to influence the study reported in this paper.

Data Availability Statement

The data for this study is available at nda.nih.gov (NDARCOL0002026 (Susan Bookheimer)).

References

Abbas, K., Liu, M., Venkatesh, M., Amico, E., Kaplan, A. D., Ventresca, M., . . . Goñi, J. (2021). Geodesic distance on optimally regularized functional connectomes uncovers individual fingerprints. *Brain Connectivity*.

Barber, A. D., Caffo, B. S., Pekar, J. J., & Mostofsky, S. H. (2013). Developmental changes in within-and between-network connectivity between late childhood and adulthood. *Neuropsychologia, 51*(1), 156-167.

Cicchetti, D. V., & Sparrow, S. A. (1981). Developing criteria for establishing interrater reliability of specific items: applications to assessment of adaptive behavior. *American journal of mental deficiency*.

Fair, D. A., Dosenbach, N. U., Church, J. A., Cohen, A. L., Brahmbhatt, S., Miezin, F. M., . . . Schlaggar, B. L. (2007). Development of distinct control networks through segregation and integration. *Proceedings of the National Academy of Sciences, 104*(33), 13507-13512.

Finn, E. S., Shen, X., Scheinost, D., Rosenberg, M. D., Huang, J., Chun, M. M., . . . Constable, R. T. (2015). Functional connectome fingerprinting: identifying individuals using patterns of brain connectivity. *Nature neuroscience, 18*(11), 1664-1671.

Forsyth, J. K., McEwen, S. C., Gee, D. G., Bearden, C. E., Addington, J., Goodyear, B., . . . Olvet, D. M. (2014). Reliability of functional magnetic resonance imaging activation during working memory in a multi-site study: analysis from the North American Prodrome Longitudinal Study. *Neuroimage, 97*, 41-52.

Gao, W., Alcauter, S., Elton, A., Hernandez-Castillo, C. R., Smith, J. K., Ramirez, J., & Lin, W. (2015). Functional network development during the first year: relative sequence and socioeconomic correlations. *Cerebral cortex, 25*(9), 2919-2928.

Gao, W., Alcauter, S., Smith, J. K., Gilmore, J. H., & Lin, W. (2015). Development of human brain cortical network architecture during infancy. *Brain Structure and Function, 220*(2), 1173-1186.

Gao, W., Lin, W., Grewen, K., & Gilmore, J. H. (2017). Functional connectivity of the infant human brain: plastic and modifiable. *The Neuroscientist, 23*(2), 169-184.

Gee, D. G., McEwen, S. C., Forsyth, J. K., Haut, K. M., Bearden, C. E., Addington, J., . . . Cornblatt, B. A. (2015). Reliability of an fMRI paradigm for emotional processing in a multisite longitudinal study. *Human brain mapping, 36*(7), 2558-2579.

Holland, D., Chang, L., Ernst, T. M., Curran, M., Buchthal, S. D., Alicata, D., . . . Yamakawa, R. (2014). Structural growth trajectories and rates of change in the first 3 months of infant brain development. *JAMA neurology, 71*(10), 1266-1274.

Horien, C., Noble, S., Finn, E. S., Shen, X., Scheinost, D., & Constable, R. T. (2018). Considering factors affecting the connectome-based identification process: Comment on Waller et al. *Neuroimage, 169*, 172-175.

Horien, C., Shen, X., Scheinost, D., & Constable, R. T. (2019). The individual functional connectome is unique and stable over months to years. *Neuroimage, 189*, 676-687.

Jalbrzikowski, M., Lei, F., Foran, W., Calabro, F., Roeder, K., Devlin, B., & Luna, B. (2019). Cognitive and default mode networks support developmental stability in functional connectome fingerprinting through adolescence. *BioRxiv*, 812719.

Joshi, A., Scheinost, D., Okuda, H., Belhachemi, D., Murphy, I., Staib, L. H., & Papademetris, X. (2011). Unified framework for development, deployment and robust testing of neuroimaging algorithms. *Neuroinformatics, 9*(1), 69-84.

Kaufmann, T., Alnæs, D., Doan, N. T., Brandt, C. L., Andreassen, O. A., & Westlye, L. T. (2017). Delayed stabilization and individualization in connectome development are related to psychiatric disorders. *Nature neuroscience, 20*(4), 513-515.

Kipping, J. A., Tuan, T. A., Fortier, M. V., & Qiu, A. (2017). Asynchronous development of cerebellar, cerebello-cortical, and cortico-cortical functional networks in infancy, childhood, and adulthood. *Cerebral cortex, 27*(11), 5170-5184.

Kolskår, K. K., Alnæs, D., Kaufmann, T., Richard, G., Sanders, A.-M., Ulrichsen, K. M., . . . Westlye, L. T. (2018). Key brain network nodes show differential cognitive relevance and developmental trajectories during childhood and adolescence. *Eneuro, 5*(4).

Lee, T.-H., & Telzer, E. H. (2016). Negative functional coupling between the right fronto-parietal and limbic resting state networks predicts increased self-control and later substance use onset in adolescence. *Developmental Cognitive Neuroscience, 20*, 35-42.

Mantel, N. (1967). The detection of disease clustering and a generalized regression approach. *Cancer research, 27*(2 Part 1), 209-220.

Mitra, A., Snyder, A. Z., Tagliazucchi, E., Laufs, H., Elison, J., Emerson, R. W., . . . Dager, S. (2017). Resting-state fMRI in sleeping infants more closely resembles adult sleep than adult wakefulness. *PloS one, 12*(11), e0188122.

Noble, S., Scheinost, D., & Constable, R. T. (2019). A decade of test-retest reliability of functional connectivity: A systematic review and meta-analysis. *Neuroimage, 203*, 116157.

Noble, S., Spann, M. N., Tokoglu, F., Shen, X., Constable, R. T., & Scheinost, D. (2017). Influences on the test–retest reliability of functional connectivity MRI and its relationship with behavioral utility. *Cerebral cortex, 27*(11), 5415-5429.

Peters, S., Van Duijvenvoorde, A. C., Koolschijn, P. C. M., & Crone, E. A. (2016). Longitudinal development of frontoparietal activity during feedback learning: Contributions of age, performance, working memory and cortical thickness. *Developmental Cognitive Neuroscience, 19*, 211-222.

Scheinost, D., Kwon, S. H., Lacadie, C., Vohr, B. R., Schneider, K. C., Papademetris, X., . . . Ment, L. R. (2017). Alterations in anatomical covariance in the prematurely born. *Cerebral cortex, 27*(1), 534-543.

Scheinost, D., Kwon, S. H., Shen, X., Lacadie, C., Schneider, K. C., Dai, F., . . . Constable, R. T. (2016). Preterm birth alters neonatal, functional rich club organization. *Brain Structure and Function, 221*(6), 3211-3222.

Shavelson, R. J., Baxter, G. P., & Gao, X. (1993). Sampling variability of performance assessments. *Journal of educational Measurement, 30*(3), 215-232.

Shrout, P. E., & Fleiss, J. L. (1979). Intraclass correlations: uses in assessing rater reliability. *Psychological bulletin, 86*(2), 420.

Vendetti, M. S., & Bunge, S. A. (2014). Evolutionary and developmental changes in the lateral frontoparietal network: a little goes a long way for higher-level cognition. *Neuron, 84*(5), 906-917.

Venkatesh, M., Jaja, J., & Pessoa, L. (2020). Comparing functional connectivity matrices: A geometry-aware approach applied to participant identification. *Neuroimage, 207*, 116398.

Wang, Y., Hinds, W., Duarte, C. S., Lee, S., Monk, C., Wall, M., . . . Mamin, M. G. (2020). Intra-session test-retest reliability of functional connectivity in infants. *BioRxiv*.

Zhang, H., Shen, D., & Lin, W. (2019). Resting-state functional MRI studies on infant brains: a decade of gap-filling efforts. *Neuroimage, 185*, 664-684.